A LONG TERM FIELD EXPERIMENT FOR RADIATIVE TRANSFER MODEL DEVELOPMENT AND LAND SURFACE PROCESSES REMOTE SENSING

Hui LU[1], Toshio KOIKE[2], Hiroyuki TSUTSUI[1], David Ndegwa KURIA[3], Tobias GRAF[1], Kun YANG[4] and Xin LI[5]

[1]Member of JSCE, Ph.D., Researcher, Dept. of Civil Eng., Univ. of Tokyo (Bunkyo-ku, Tokyo 113-8656, Japan)
[2]Member of JSCE, Dr. Eng., Professor, Dept. of Civil Eng., Univ. of Tokyo (Bunkyo-ku, Tokyo 113-8656, Japan)
[3] Doctoral Student, Dept. of Civil Eng., Univ. of Tokyo (Bunkyo-ku, Tokyo 113-8656, Japan)
[4] Member of JSCE, Ph.D., Professor, Inst. of Tibet, CAS (Beijing 100085, China)
[5]Ph.D., Professor, Cold and Arid Regions Envi. and Eng. Research Inst., CAS (Lanzhou 730000, China)

From November 2006 to June 2007 a field experiment 'Tanashi Experiment' was conducted in a farm of the University of Tokyo, Japan. The scientific objectives are presented in this paper and the corresponding experiment set-up is described. The influences of soil moisture and vegetation layer on the brightness of various frequencies are analyzed. The sensitivity of higher frequencies on the soil moisture changing is identified. The TB of all frequencies and polarization is found to be saturated and reach same values when vegetation water content larger than 4 kg/m^2. A Land Data Assimilation System developed by the University of Tokyo (LDAS-UT) is validated by using data obtained from this experiment. And one important merit of LDAS-UT, parameter optimization, is verified through the comparison of optimized parameters with the in situ observed ones. The difference between the optimized parameters and the observed 'real' ones reveals the potential source of uncertainty in the system due to the limitation of current Radiative Transfer Model (RTM) and Land Surface Scheme (LSS).

Key Words**:** *Ground Based Passive Microwave Radiometer, Soil Moisture, Microwave Remote Sensing, Vegetation Effects, Land Data Assimilation System, Parameters Optimization*

1. INTRODUCTION

Researches related to earth system modeling, global scale environmental processes monitoring and climate changing studying are conducted using globally measured parameters, such as the soil moisture, soil temperature and vegetation water content. Among them, the primary one is the soil moisture, which links the land surface and atmosphere by influencing the exchange of energy and material between these two parts. However, due to its large variability, it is very difficult to observe the spatial and temporal distribution of soil moisture in a large scale by in situ measurements, which are both time consuming and expensive. As a result, in recent 30 years, much effort has been directed towards observing soil moisture by satellite remote sensing approaches. Fortunately, satellite passive microwave remote sensing offers a possibility to measure such an important variable at the global scale, by directly measuring the dielectric properties which are strongly related to the liquid moisture content. Moreover, extra advantages of passive microwave remote sensing include long wavelength in microwave region and independent of illumination source. These characteristics have been recognized by many scientists and large research activities have been carried out in the past 30 years.

Currently, globally soil moisture products are mainly retrieved from C band and X band observation[1)]. And in order to get time continuous information about soil moisture and land surface energy budget, land surface data assimilation systems are developed. But there are still some problems left to be solved, such as retrieval soil moisture from higher frequency bands (19GHz and 37GHz) observation, counting the vegetation effects on different frequencies, and the parameterization problems inside the land data assimilation systems.

In order to improve our understanding of the radiative transfer process taken place on the land surface and to improve our capability to model land

surface processes, a long term field experiment was designed to monitor the growth cycle of winter wheat, and have been carried out from November 2006 to June 2007 in the Field Production Science Center in Graduate School of Agricultural and Life Sciences in the University of Tokyo (UTFPSC), Tokyo, Japan.

In this paper, we present the objectives and the overall set-up of the 'Tanashi experiment'. Some radiometric characteristics of bare soil and winter wheat were explored through microwave observations at the frequencies operating by the Advanced Microwave Scanning Radiometers for EOS (AMSR-E) (6.925GHz, 10.65GHz, 18.7GHz, 23.8GHz, 36.5GHz and 89GHz). Finally the LDAS-UT was driven by the observed meteorological forcing data. The parameter optimization capability of LDAS-UT is validated through comparing retrieved land parameters with the observed ones.

2. EXPERIMENT DESCRIPTION

The 'Tanashi Experiment' was designed with the following two objectives in mind: (1) Improving the understanding of the influences of soil and vegetation on the remote sensing signals at different frequencies and polarizations; and (2) Improving the understanding of the interaction processes between land surface and atmosphere, through the validation of LDAS-UT with in situ observed data set.

(1) Site Overview

Fig. 1 provides an overview of the instrument set-up. Two Ground Based Microwave Radiometer (GBMR) systems, GBMR-6ch and GBMR-7ch, have been installed at the edge of experiment field. In front of those two radiometers, there are 5 footprints which are the main targets of this field experiment.

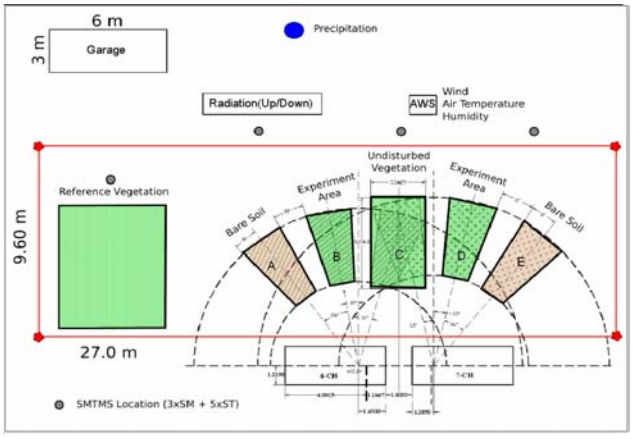

Fig. 1 Overview of Instrument Set-Up

The footprint A and B are the reference bare soil footprint and reference vegetation footprint of GBMR-6ch, respectively. Analogously, footprint E and D are the reference footprints for the another radiometer, i.e. GBMR-7ch. The footprint C, the one in the central location which can be observed by GBMR-6ch and GBMR-7ch simultaneously, is the common footprint.

Two different scan areas have been selected to observe the brightness temperature of field in different situations:

Footprint B,C and D – Undisturbed footprint: The plots in this area were undisturbed during whole observation period and therefore it represented the natural status of the field.

Footprint A and E – Reference bare soil footprint: In this area the vegetation was removed regularly to keep the bare soil exposed to radiometers.

Beside those 5 footprints, there is a plot used as vegetation reference site. All of the vegetation sampling procedures were taken here to avoid disturb the natural situation of footprint B, C and D.

The location for soil moisture and temperature measurement system (SMTMS) and the automatic weather station (AWS) have been selected, so that they are close to the radiometer footprints. The radiation station and rainfall gauge are also located close to the footprint to ensure the representativity of meteorological data measurement.

(2) Brightness Temperature Observation

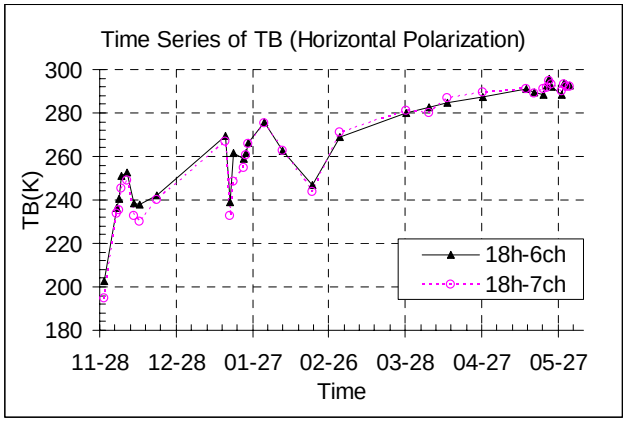

Fig. 2 Comparison of TB observed at 18GHz by GBMR-6ch and GBMR-7ch

The ground based brightness temperature observations have been implemented by means of the 6 channel Ground Based Microwave Radiometer (GBMR-6ch) and 7 channel Ground Based Microwave Radiometer (GBMR-7ch). The GBMR-6ch is a dual polarization, multi-frequency passive microwave radiometer, which observes the brightness temperature at 6.925, 10.65 and 18.7 GHz, while the GBMR-7ch operating at frequencies of 18.7, 23.8, 36.5 and 89GHz with both horizontal and vertical polarizations, with the exception of 23.8GHz which is vertical polarization only. The set of those two radiometers was developed to provide frequencies similar to those of the Advanced Microwave Scanning Radiometers for EOS

(AMSR-E) on Aqua and AMSR on ADEOS-II. Details of GBMR-6ch and GBMR-7ch can be found from a former paper of authors[2)] and from manuals provided by the manufacturer, RPG[3)].

Fig.2 shows a comparison between the brightness temperatures observed at 18.7 GHz by GBMR-6ch and that by GBMR-7ch. The line with triangle represents the results measured by GBMR-6ch, and the line with cycle is those measured by GBMR-7ch. The root mean square error between the GBMR-7ch and GBMR-6ch is 1.74K for vertical polarization (not shown here), and 4.03K for horizontal polarization, respectively. Considering the fact that the calibration scheme is different for GBMR-6ch and GBMR-7ch, and the fact that the observed target is around 300K, the error is negligible. And then, we are sure that both systems were observing same target with same accuracy at same time. Finally, a brightness temperature data set from 6.9GHz up to 89GHz is then created.

(3) Soil temperature and moisture measurement

The Soil Moisture and Temperature Measurement System (SMTMS) was installed for simultaneous measurement of soil moisture and temperature profiles. The SMTMS used in this study have ten temperature probes and six soil moisture probes. Those probes were set at the following depths 0cm, 3 cm, 5 cm, 10 cm, 20 cm, 50 cm and 100 cm.

Soil samples were taken after every measurement to obtain the soil density and water content. The infrared thermometer was used for the measurement of soil surface temperature and vegetation surface temperature.

(4) Meteorological data measurement

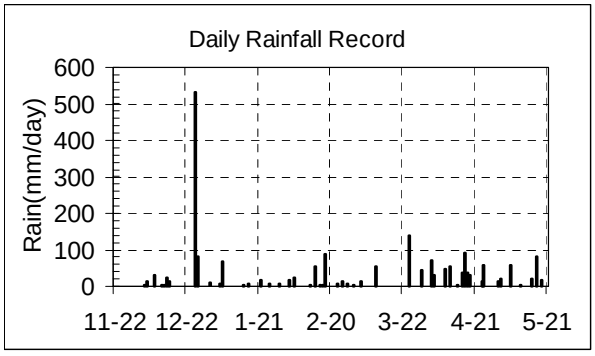

Fig. 3 Time series of daily rainfall

The automated weather station (AWS) was installed to continuously monitor the meteorological conditions at the site. The following items were recorded by AWS every 10 minute: wind direction, wind speed, air temperature, relative humidity, radiation (upward and downward of long wave and shortwave) and precipitation. Those atmospheric measurements are used to drive the Land Surface Data Assimilation System of the University of Tokyo (LDAS-UT).

Fig.3 shows a time series of daily rainfall. It can be identified easily that a typhoon hit this field at December 26 2006 and brought a heavy rain of 531 mm. This extreme event changed the soil moisture content and surface roughness dramatically, and it also destroyed the TDR probes and we lost continuous soil moisture profile measurement.

(5) Soil texture and roughness data

The soil in the field is so-called 'Kanto loam', a typical soil in Tokyo area, with a sand fraction of 26% and a clay fraction of 43%. The observed soil bulk density is 0.587 g/cm3 for the period before February 2007 and 0.606 for period from March to June 2007.

The land surface roughness was measured by a roughometer. Two roughness parameters *rms* height (h) and correlation length (l) were retrieved from roughness measurement. Since we can not go into the field after winter wheat well developed, there is not roughness measurement for vegetated plots after February.

(6) Vegetation measurement

Vegetation development was monitoring through measuring the height, biomass, dry matter, water content and LAI. Sampling area of 1*1 m^2 area was selected in the vegetation reference field. Wet biomass was measured just after cutting, and then the wheat was separated into three parts: heads, leaves and stems. Weight and area of each part were measured separately. By summing the area of those three parts, the Leaf Area Index (LAI) was calculated.

A spectroradiometer, ASD FieldSpec Pro, was also used to measure the reflectance at a spectral range of 350nm – 2500nm. The normalized difference vegetation index (NDVI) was calculated by using reflectance values of red bands (620 - 670nm) and Near-Infrared (NIR) bands (841 - 876 nm), the same bands as MODIS products using.

According to the field observation, the vegetation water content (VWC) increased slowly during the period from November to March. And after March, the vegetation developed rapidly. The whole experiment therefore can be divided into two periods: no vegetation effects period (before March) and vegetated period (after March 28).

3. OBSERVED RESULTS OF FIELD EXPERIMENTS

Observation results are presented in this section. They focus on the new possibilities offered by the multi-frequency observation of the whole vegetation development process. First, the variability of brightness temperature to the variation of soil

moisture is analyzed, from low frequency of 6.9GHz up to the high frequency of 89GHz. Then the vegetation effects on different frequency observation are analyzed.

(1) Soil moisture influents on the brightness temperature of different frequencies

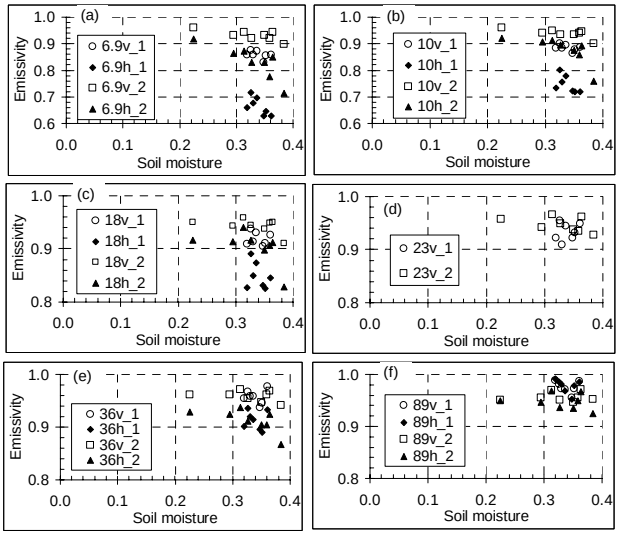

Fig. 4 Variation of emissivity at different frequencies according to the change of soil moisture, for no vegetation effects period

Fig. 4 shows the observed apparent emissivity (equals to the observed brightness temperature divided by the surface temperature) changing with various soil moisture content, for no vegetation effects period. The observation frequency of each panel is shown in the legend, for example, "6.9v_1" represents the observation at 6.9 GHz vertical polarization during the first period (before the typhoon), where "_2" means the observation during the second period (after the typhoon).

As mentioned in section 2.4, the typhoon changed the soil moisture and surface roughness dramatically. As a result of it, the emissivity of low frequencies (6.925GHz, 10GHz and 18GHz) is separated into two groups (group 1 before typhoon and group 2 after typhoon). And the emissivity is increased after typhoon occurred. Such situation is more obvious for horizontal polarization than for vertical polarization. This can be explained that the horizontal signals are more sensitive to the surface roughness than the vertical ones do.

From **Fig. 4**, it is easy to identify that the observed emissivity decreases as soil moisture increases for all horizontal polarization cases. This finding confirms previous studies[4, 5] and is in good agreement with the radiative transfer theory which builds on the basis of Dobson model and Fresnel equation for the wet soil cases[6-8].

Table 1 shows the decrement of the observed apparent emissivity due to the soil moisture increasing from 0.22 to 0.38. The decrement of emissivity is different for different frequencies and polarizations, with larger decrement for lower frequencies. From this table, it is obviously that lower frequencies and horizontal polarization are sensitive to the soil moisture changing. This finding provides a strong support to use lower frequencies of AMSR-E to observe soil moisture from space. Moreover, it is also found that there also exists some sensitivity for higher frequencies to the soil moisture changing. This means it is possible to retrieve soil moisture from high frequencies observation, such as data of SSM/I and WindSat. Then long term global soil moisture date can be estimated from long term SSM/I data to benefit researches related to the climate change and global warming.

Table. 1 Decrement of apparent emissivity due to the soil moisture increasing from 0.22 to 0.38

Pola. / F(GHz)	Vertical Polarization	Horizontal Polarization
6.925	0.06	0.21
10.65	0.06	0.16
18.7	0.04	0.09
23.8	0.03	
36.5	0.02	0.06
89	0.00	0.02

(2) Vegetation effects on the brightness temperature of different frequencies

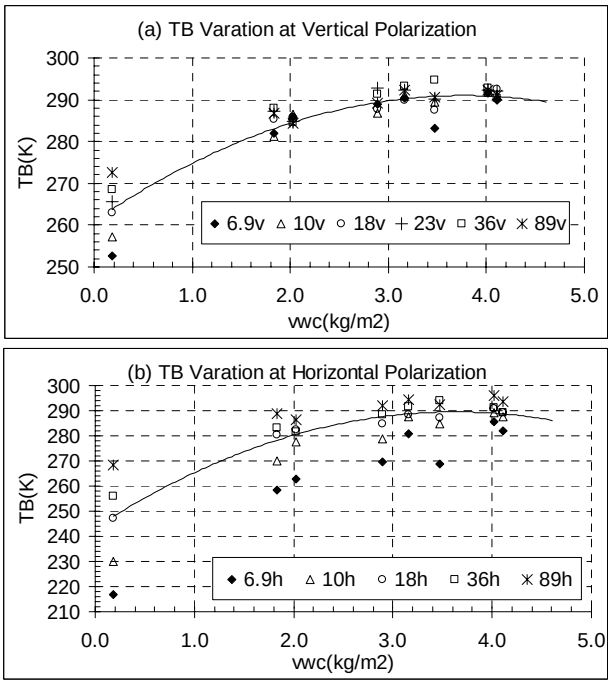

Fig. 5 Brightness temperature responsive to the vegetation water content

Fig. 5 Shows the changes of the brightness temperature due to the increase of vegetation water content. From **Fig. 5,** it is obviously that the

brightness temperature is increasing as vegetation water content increasing. And finally, it gets saturated and all frequencies and polarizations give almost same values. For the cases of small VWC (such as vwc = 0.182 kg/m^2), the difference of brightness temperature for different frequencies is large, giving 89GHz with largest values and 6.9GHz with smallest values. But for the cases of VWC larger than 2.0, it is hard to find such difference for vertical polarization case. For more vegetation water cases, all frequencies and polarizations observe almost same values. By comparing panel (a) with (b), it is clear that the emission from vegetation layer is becoming dominant at vertical polarization earlier than at horizontal one.

By using Jackson's model[9], we can calculate the optical thickness (τ) and transmittivity (L) of vegetation layer as following equations:

$$\tau = b' \times \lambda^{\chi} \times VWC \quad (1)$$

$$L = \exp(-\tau / \cos\theta) \quad (2)$$

where λ is wavelength in cm, VWC is vegetation water content in kg/m^2, θ is incident angle. b' and χ are parameters dependent on the vegetation type. In the case of winter wheat, they are equal to 1.15 and -1.08, respectively.

Table. 2 Transmittivity of vegetation layer

Date	Feb-07	Mar-28	Apr-13	May-17
VWC (kg/m^2) / F(GHz)	0.084	1.834	2.894	4.109
6.925	0.97	0.47	0.30	0.18
10.65	0.95	0.30	0.15	0.07
18.7	0.90	0.11	0.03	0.01
23.8	0.88	0.06	0.01	0.00
36.5	0.81	0.01	0.00	0.00
89	0.58	0.00	0.00	0.00

Table 2 shows the calculation results of the transmittivity of vegetation layer at the date of February 7, March 28, April 13 and May 17. From **Table 2**, it is clear that the vegetation effect is small at February 7, giving the facts that the transmittivity is larger than 0.9 for lower frequencies. And after March 28, transmittivity is less than 0.5 for all frequencies. By summarizing results shown in Fig. 5 and table 2, the heavy vegetation criterion, over which the emission from vegetation layer is uniform for all microwave frequencies and polarization, is 2 kg/m^2 for frequencies higher than 18.7GHz. For all frequencies equipped on AMSR-E (including 6.925 and 10.65GHz), this criterion should move to 4.0kg/m^2.

4. VALIDATION OF LDAS-UT

As introduced in section 2, one of the main objectives of this long term experiment is to study the interaction between land surface and atmosphere. To accomplish this target, we run LDAS-UT[10] to simulate soil variables (moisture and temperature profiles) and surface energy budget, by using in situ observed meteorological data as forcing data and GBMR TB data as observation data. As introduced by Yang et al. [10], one important merit of LDAS-UT is its capability to optimize surface parameters by only using meteorological data and Brightness Temperature (TB) data. We therefore run LDAS-UT in two scenarios: one running with in situ observed surface parameters and another running with optimized parameters produced by LDAS-UT itself.

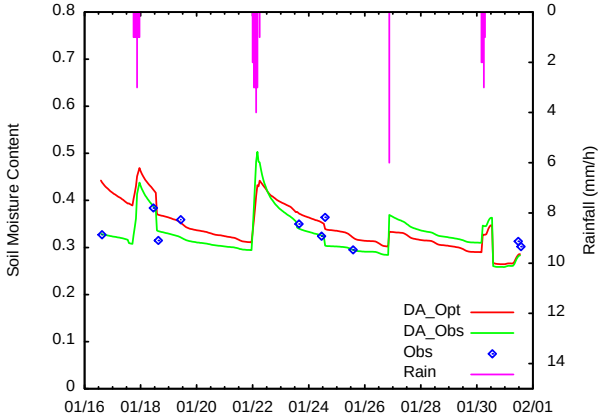

Fig. 6 Comparison between assimilated soil moisture and in situ observed one

Fig. 6 shows a comparison between assimilated soil moisture and in situ observed one. The red line, marked as "DA_Opt", represents the assimilated results by using optimized parameters; the Green line, marked as "DA_Obs", represents the simulation result by using observed parameters; the cycles, marked as "Obs", are the in situ soil moisture observed by can samples; and the purple columns represent the hourly rainfall. It is clear that both simulation scenarios are in good agreement with the field observation, while the simulation with optimized parameter estimates soil moisture a little higher than the simulation with observed parameters does. This overestimation is due to the setting of initial soil moisture values. For observed parameters simulation case, the observed soil moisture was used as initial value, while the initial value is much larger for optimized parameter simulation case. The RMSE of optimized parameter simulation is 0.045 and a little larger than that of observed parameter simulation which is 0.026.

Table 3 shows a comparison between optimized parameters and observed parameters. Generally speaking, the different between two sets of parameter is not so large. The optimized soil texture parameters are very close to the observed ones. It means that models use for accounting soil texture

effects in LDAS-UT are in good agreement with physical truth. The optimized porosity is smaller than the observed one. It may be due to the measurement errors which overestimate the porosity or due to the limitation of current models in which the organic materials are not accounted. And same situation is faced for the roughness parameters case. The difference between the optimized parameters and the observed ones reveals the potential source of uncertainty in the system due to the limitation of current RTM and LSS. And more detailed researches are needed to address on those parameters.

Table. 3 Comparison between optimized parameters and observed parameters

	Optimized	Observed
SAND (%)	28.3	26
CLAY (%)	34.9	43
Porosity	0.587	0.778
rms *h* (cm)	0.513	1.01
l (cm)	0.478	1.16
www1	0.45	0.327

NOTE: www1 represents the soil moisture content of the first soil layer in SiB2 (0-5cm)

5. SUMMARY

The 'Tanashi Experiment' is the first long term field experiment with TB measurement at all frequencies equipped on AMSR-E. 'Tanashi Experiment' was designed to couple the land surface process study and microwave radiative transfer model development, simultaneously. The data set made by this experiment provides us an opportunity to study the land surface radiative transfer process at various frequencies. And it also can be used to validate land surface scheme and data assimilation system.

From the no vegetation effects period, the observation results at lower frequencies are in accordance with former studies. Moreover, it is found that the higher frequencies also have some sensitivity to the soil moisture variation. This new finding encourages us to retrieve soil moisture from high frequencies observation data set, such as SSM/I and WindSat. Through analyzing the experiment results at vegetated period, the vegetation effects on various frequencies were studied. It is found that the heavy vegetation criterion is 2.0 kg/m^2 for frequencies higher than 18 GHz and is 4.0 kg/m^2 for all AMSR-E frequencies.

By using in situ observed meteorological forcing data and TB data observed by GBMR, the capability of LDAS-UT was validated with the fact that its soil moisture estimation is in good agreement with in situ observation, whatever using observed parameters or optimized parameters. The difference between the optimized parameters and the observed ones reveals the potential source of uncertainty in the system, which should be addressed further.

ACKNOWLEDGMENT:

This study was carried out as part of the Coordinated Enhanced Observing Period (CEOP) and Verification Experiment for AMSR/AMSR-E funded by the Japanese Science and Technology Corporation for Promoting Science and Technology Japan and the Japan Aerospace Exploration Agency. The authors express their great gratitude to them.

Furthermore we would like to thank UTFPSC, for providing us the possibility to conduct the field experiments in the university farm, Prof. Yonegawa and Mr. Kuboda for his helping in field management.

REFERENCES

1) Eni G. Njoku, Thomas J. Jackson, Venkataraman Lakshmi, Tsz K. Chan., and Son V. Nghiem: Soil Moisture Retrieval From AMSR-E, *IEEE Trans. Geosci. Remote Sensing*, vol 41, pp. 215-229, February, 2003.
2) Hui Lu, Toshio Koike, et al: A Basic Study on Soil Moisture Algorithm Using Ground-Based Observations under Dry Condition, JSCE, Vol. 50, Feb. 2006
3) Technical documents of Radiometer Physics GmbH: Description 6 channel radiometer, Meckenheim, Germany. May, 1996
4) E. G. Njoku, "Theory for Passive Microwave Remote-Sensing of near-Surface Soil-Moisture," Journal of Geophysical Research, vol. 82, pp. 3108-3118, 1977.
5) T. J. Jackson, P. E. ONeill, and C. T. Swift, "Passive microwave observation of diurnal surface soil moisture," Ieee Transactions on Geoscience and Remote Sensing, vol. 35, pp. 1210-1222, 1997
6) Ulaby, F. T., Moore, K. T. and Fung, A. K.: *Microwave Remote Sensing: Active and Passive, Volume III: From Theory to Application*, Artech House Publishers, 1986
7) M. C. Dobson, F. T. Ulaby, M. T. Hallikainen, and M. A. El-Rayes: Microwave Dielectric Behavior of Wet Soil—Part II: Dielectric Mixing Models, *IEEE Trans. Geosci. Remote Sensing*, vol. GE-23, No. 1, pp. 35-46, January, 1985.
8) P. S. Ray: Broadband Complex Refractive Indices of Ice and Water, *Applied Optics*, vol. 11, No. 8, pp. 1836-1844, August, 1972
9) T. J. Jackson and T. J. Schmugge: Vegetation Effects on the Microwave Emission of Soils, *Remote Sens. Environ*., Vol. 36, pp. 203-212, 1991.
10) Kun YANG, Takahiro WATANABE, et al: An Auto-calibration System to Assimilate AMSR-E data into a Land Surface Model for Estimating Soil Moisture and Surface Energy Budget, *JMSJ*, Vol. 85A, pp 229-242, 2007.

.

(Received September 30, 2007)